THE JOURNAL OF PHYSICAL CHEMISTRY B

Article

Cite This: J. Phys. Chem. B XXXX, XXX, XXX-XXX

pubs.acs.org/JPCB

Development of a ReaxFF Force Field for Cu/S/C/H and Reactive MD Simulations of Methyl Thiolate Decomposition on Cu (100)

Jejoon Yeon,[†] Heather L. Adams,[‡] Chad E. Junkermeier,[§] Adri C. T. van Duin,[∥] Wilfred T. Tysoe,[‡] and Ashlie Martini*[,†]

[†]Department of Mechanical Engineering, University of California, Merced, California 95343, United States

[‡]Department of Chemistry and Laboratory for Surface Studies, University of Wisconsin-Milwaukee, Milwaukee, Wisconsin 53211, United States

[§]Research Corporation of the University of Hawaii, Honolulu, Hawaii 96848, United States

[∥]Department of Mechanical and Nuclear Engineering, The Pennsylvania State University, University Park, Pennsylvania 16802, United States

Supporting Information

ABSTRACT: It has been shown that the rate of decomposition of methyl thiolate species on copper is accelerated by sliding on a methyl thiolate covered surface in ultrahigh vacuum at room temperature. The reaction produces small gas-phase hydrocarbons and deposits sulfur on the surface. Here, a new ReaxFF potential was developed to enable investigation of the molecular processes that induce this mechanochemical reaction by using density functional theory calculations to tune force field parameters for the model system. Various processes, including volumetric expansion/compression of CuS, CuS_2, and Cu_2S unit cells; bond dissociation of Cu−S and valence angle bending of Cu−S−C; the binding energies of SCH_3, CH_3, and S atoms on a Cu surface; and energy for the decomposition of methyl thiolate molecular species on copper, were used to identify the new ReaxFF parameters. Molecular dynamics simulations of the reactions of adsorbed methyl thiolate species at various temperatures were performed to demonstrate the validity of the new potential and to study the thermal reaction pathways. It was found that reaction is initiated by C−S bond scission, consistent with experiments, and that the resulting methyl species diffuse on the surface and combine to desorb ethane, also as found experimentally.

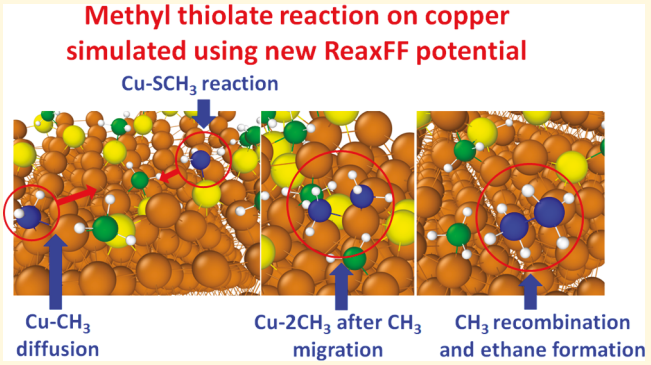

INTRODUCTION

Copper is used for a range of technological applications, for example, as a catalyst,[1] for electrodes in fuel cells,[2] and in electrical motors.[3] Although coinage metals are generally quite unreactive, they can be passivated by sulfur-containing alkyl thiolate self-assembled monolayers,[4−6] and the chemisorption of other molecules has been investigated.[7−9]

Sulfur-containing molecules are also used as lubricant additives, where they react at the sliding interface to form friction- and/or wear-reducing films.[6,10−12] Early mechanistic work on sulfur-containing lubricant additives under so-called extreme-pressure (EP) conditions, where the interfacial temperatures were high (approaching ∼1000 K),[13] revealed that the surface chemical processes that resulted in the formation of friction-reducing tribofilms were thermally driven.[14−18] However, in the case of milder sliding conditions, where the temperature rise at the interface is negligible, the formation of a tribofilm can be driven by a mechanochemical process in which interfacial sliding lowers the reaction activation barrier, resulting in an acceleration of the reaction rate.[19−21] In particular, this effect has been demonstrated for the gas-phase lubrication of copper by dialkyl disulfides (R−S−S−R, where R is an alkyl group).[22−27] The dialkyl disulfides initially reacted rapidly on clean, well-characterized copper in ultrahigh vacuum (UHV) to form stable alkyl thiolate species. However, sliding on this surface induced the decomposition of the alkyl thiolate species to evolve gas-phase hydrocarbons and deposit sulfur on the surface. It is important to note that this reaction would not occur in the absence of an external force, and that the sliding conditions were sufficiently mild that the interfacial temperature rise during siding was negligible; the reaction rate was mechanochemically accelerated.

Such mechano- or tribochemical reactions are generally most simply described using the so-called Bell model[28] where the reaction rate constant under the influence of an external force F

Special Issue: Miquel B. Salmeron Festschrift

Received: July 15, 2017
Revised: October 3, 2017
Published: October 5, 2017

DOI: 10.1021/acs.jpcb.7b06976
J. Phys. Chem. B XXXX, XXX, XXX−XXX

exerted on the reacting species (the mechanophore), $k(F)$ is given by

$$k(F) = k_0 \exp\left(\frac{F\Delta x^{\ddagger}}{k_B T}\right) \quad (1)$$

where k_0 is the reaction rate constant in the absence of an external force, k_B is the Boltzmann constant, T the absolute temperature, and $\Delta x^{\ddagger}$ is known as the activation length and is a measure of the distance moved along the reaction energy profile from the reactant to the transition state.[29] However, it is a challenge to quantitatively test this model for a number of reasons. First, this model assumes that the shape of the reaction profile is not modified by the imposition of an external force, and thus is somewhat oversimplified.[30] It also assumes that the external force is collinear with the reaction coordinate, which it may well not be. Molecular dynamics (MD) simulations have proven to be extremely useful in providing atomic-scale insights into energy dissipation processes at a sliding interface, and have more recently been extended to studying chemical reactions at interfaces by using reactive potentials that include bond-breaking and bond-forming processes.[31−33] While there remain a number of challenges to modeling chemical processes using MD simulations, they can provide important molecular-level insights into the processes occurring at a sliding interface that can aid in developing robust analytical models analogous to the Bell model described above, and in providing physical insights into the value of parameters, such as the activation length.

The first challenge to applying MD simulations to mechano- and tribochemical processes is to develop reasonably accurate interaction potentials. This is done in the following by using density functional theory (DFT) calculations as a basis for fitting the parameters in a ReaxFF reactive force field,[34,35] and previous work has shown that DFT calculations yield energy barriers for the decomposition of methyl thiolate species on copper that are in good agreement with experiment.[22] A second challenge in using MD simulations to study chemical reactions is that they are relatively rare events on the MD time scale. This can be addressed, in some cases, by using accelerated parallel replica dynamics.[36−40]

Since there were no ReaxFF parameters for the methyl thiolate species on copper system, in this work, new ReaxFF parameters were developed to describe the Cu−S and Cu−thiolate reaction energetics. The new ReaxFF force field was trained, that is the parameters in the potential were optimized, by using DFT calculations of the volumetric expansion/compression of CuS, CuS_2, and Cu_2S unit cells; Cu−S bond dissociation; the Cu−S−C valence angle bending; the binding energies of SCH_3, CH_3, and S species on copper; and the potential energy curves for the decomposition of methyl thiolate on Cu (100). The resulting ReaxFF potential was then used in preliminary MD simulations of the decomposition of methyl thiolate species at various temperatures, which were compared with experiment to demonstrate the ability of the newly developed force field to model the methyl thiolate decomposition pathways on Cu (100).

METHODS

ReaxFF Formalism. ReaxFF is an empirical reactive force field that can simulate relatively large atomic systems with an accuracy comparable to DFT or other quantum-based methods, but with much less computational time.[34,41] ReaxFF calculates the partial energies of the system and the total energy for every iteration during the simulation using the following equation:

$$E_{system} = E_{bond} + E_{under} + E_{over} + E_{val} + E_{tor} + E_{lp} + E_{vdw} + E_{Coul} \quad (2)$$

where the partial energies are bond, under-coordination correction, overcoordination penalty, valence angle, dihedral angle, lone-pair electron, van der Waals interaction, and Coulomb interaction energies, respectively.

A bond order−bond length relationship is used to calculate atomic interactions. This enables the ReaxFF potential to simulate the transition states of bonding interactions with comparable accuracy to quantum-based methods. Bond orders in ReaxFF are calculated from the equation:

$$\begin{aligned} BO'_{ij} &= BO^{\sigma}_{ij} + BO^{\pi}_{ij} + BO^{\pi\pi}_{ij} \\ &= \exp\left[p_{bo1}\left(\frac{r_{ij}}{r^{\sigma}_{o}}\right)^{p_{bo2}}\right] + \exp\left[p_{bo2}\left(\frac{r_{ij}}{r^{\pi}_{o}}\right)^{p_{bo4}}\right] \\ &\quad + \exp\left[p_{bo5}\left(\frac{r_{ij}}{r^{\pi\pi}_{o}}\right)^{p_{bo6}}\right] \end{aligned} \quad (3)$$

where BO^{σ}_{ij}, BO^{π}_{ij}, and $BO^{\pi\pi}_{ij}$ are the bond-order contributions from σ bonds, π bonds, and double π bonds, respectively. The P_{bo} variables are the parameters used in the force field to describe bonding interactions; these variables are fit or trained during the parametrization of a new force field. r_{ij} is the atomic distance between the i^{th} and j^{th} atoms, and the various r_o values are the optimal bond radii. All interaction energies associated with bonding are functions of the BO values. Thus, because they depend on bond distances, and because the variables are trained with quantum mechanical results or experiment data, ReaxFF is able to calculate the transition-state energies of reactions with comparable accuracy to those from either DFT or experiment.

Nonbonding interactions ($E_{vdw} + E_{Coul}$ in eq 2) are calculated for every iteration, regardless of connectivity. A seventh-order taper function is used to prevent any discontinuities of energies for nonbonding interactions.[42] In addition, shielding parameters inhibit unphysically large repulsive energies at very close distances.[43] The methods used to calculate nonbonding interactions enable ReaxFF to simulate long-range, ionic interactions.[44] Furthermore, ReaxFF uses an electronegativity equalization method, a geometry-dependent charge calculation scheme, to calculate atomic charges.[45] More detailed information about the ReaxFF potential is provided in van Duin et al.,[34] and Chenoweth et al.[46]

Ab Initio Reference Data. Quantum mechanical (QM) calculations were performed to gather reference energies for calculating ReaxFF parameters. The calculations include the equations of state of CuS, CuS_2, and Cu_2S, bond-dissociation curves, valence-angle curves, thiol decomposition on a Cu(100) surface, the binding energies of S, CH_3, and thiolates on Cu(100). Molecular structures, with nonperiodic boundary conditions were calculated using the Jaguar package. Nonperiodic DFT calculations used the B3LYP functional,[47] which is based on Hartree−Fock exchange with a generalized functional by Becke,[48] and a correlational functional by Lee, Yang, and Parr.[49] The Pople 6-31G**+ basis set was applied for the calculation of the electrons of Cu, S, C, and H atoms.[50] For geometries with periodic boundary conditions, the PWSCF (Plane Wave Self Consistent Field) code in the Quantum

DOI: 10.1021/acs.jpcb.7b06976
J. Phys. Chem. B XXXX, XXX, XXX−XXX

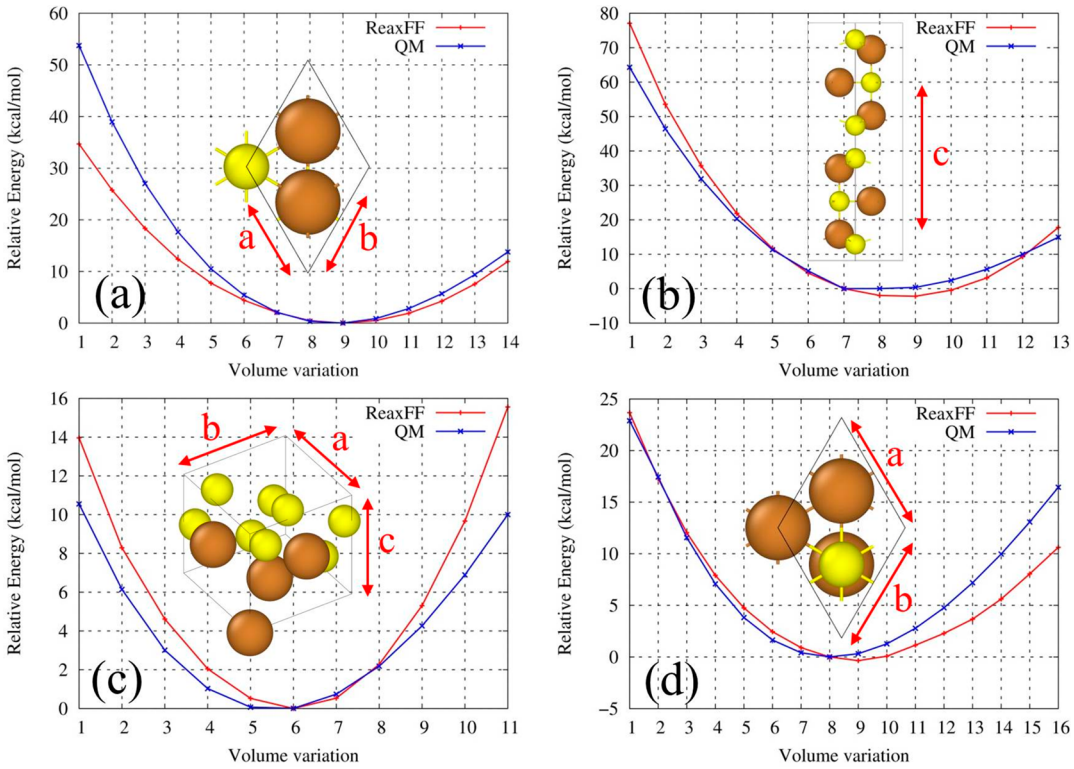

Figure 1. Energy curves for the equations of state of the (a) CuS unit cell with a volumetric variation along the lattice vectors a and b; (b) CuS unit cell with the volumetric variation along the lattice vector c; (c) CuS_2 unit cell with a volumetric variation along the lattice vectors a, b, and c; and (d) Cu_2S unit cell with a volumetric variation along the lattice vectors a and b. Insets to the plots show the unit cells, where brown spheres correspond to Cu and yellow spheres to S.

Espresso package was used,[51] with the PBE functional condition,[52] with the scalar relativistic ultrasoft pseudopotentials using the Rappe Rabe Kaxiras Joannopoulos (RRKJus)[53,54] method to describe ion-electron interactions.

Convergence test calculations were performed to find the optimal conditions for kinetic energy and charge density cutoffs; the cutoff values were set to 75 and 580 Ry, respectively. In addition, a Monkhorst–Pack grid with a 7 × 7 × 7 k-point mesh was used for the equation-of-state calculations, while a 4 × 4 × 1 k-point mesh was applied to all DFT calculations with the Cu(100) vacuum slab, and 1 × 1 × 1 mesh for the molecules.[55,56]

Parameterization Process. The initial step in the ReaxFF parametrization process for the Cu–S system was to combine previously developed ReaxFF parameters for copper[57] and sulfur.[35] Next, the subsequent parametrization process used quantum mechanics to train each parameter in eq 3. The training process optimized one parameter at a time, to minimize the sum of the errors.[41] The error was calculated from the difference between the ReaxFF and QM/experiment data as described by the following equation:

$$\text{Error} = \sum_{i}^{n} \left(\frac{x_{i,\text{QM}} - x_{i,\text{ReaxFF}}}{\sigma_i} \right)^2 \quad (4)$$

where the $x_{i,\text{QM}}$ represent the energies from quantum mechanics, $x_{i,\text{ReaxFF}}$ are the energies from ReaxFF, and σ_i are weighting values for each parameter. The resulting ReaxFF parameters are available as Supporting Information.

RESULTS AND DISCUSSION

Force-Field Parameterization. To ensure the reliability of the ReaxFF description of condensed-phase Cu–S, the equations of state for CuS, Cu_2S, and CuS_2 were calculated by DFT. The energies were calculated for these same systems using ReaxFF. For each system, the simulation began with the equilibrium state of the unit cell and then expansion and compression were applied along the relevant lattice directions for each unit cell and the energy of the system was calculated. For all equation of state calculations, the volume was varied by 2% for each step. The resulting relative energies were compared to those from DFT. The c-direction equation of state for Cu_2S was not considered in this training set because the difference between the minimum and maximum energies calculated from QM calculations was less than 1 kcal/mol; this means that expansion or compression along the c-direction is barrierless and therefore is unimportant for ReaxFF. Figure 1 shows the QM and ReaxFF results for volumetric compression and expansion, where each increment along the *x*-axis corresponds to a 2% change in unit cell volume. Within a 10% volume variation from the equilibrium state, the maximum difference between ReaxFF and QM energies was between 3.3 and 9.0 kcal/mol. Near equilibrium, i.e., for a volume expansion of 2% or less, the performance of the force field was even better, yielding a maximum energy difference between 0.6 and 1.6 kcal/mol, where all energy differences were less than 1 kcal/mol except for the CuS unit cell contracted by 2% in the lattice vector c direction.

To develop a ReaxFF description of alkyl thiolate interactions with Cu surfaces, the Cu–S bond dissociation and Cu–S–C valence-angle energies were calculated by DFT

DOI: 10.1021/acs.jpcb.7b06976
J. Phys. Chem. B XXXX, XXX, XXX–XXX

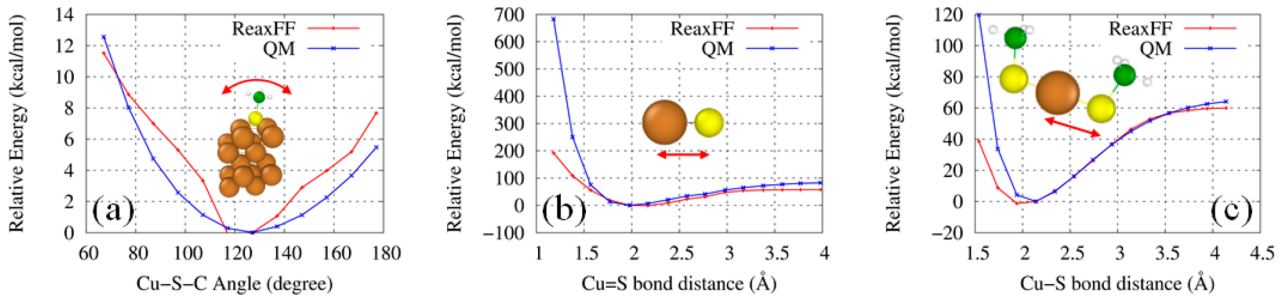

Figure 2. ReaxFF and QM energy curves for the (a) Cu−S−C angle in a Cu (100)-thiolate system, (b) Cu−S bond in thioxocopper, and (c) Cu−S bond in $Cu(SCH_3)_2$. Insets to the plots show the model systems, where brown spheres correspond to Cu, yellow to S, green to C, and white to H atoms.

and the results compared and trained with ReaxFF. Bond dissociation for Cu−S was calculated using thioxocopper (CuS) and a $Cu(SCH_3)_2$ molecule, and valence-angle calculations of Cu−S−C were carried out using the Cu (100)-methyl thiolate system. In all cases, geometry optimizations were performed to find the ground-state energies of each system. To calculate the energy curve for Cu−S bond dissociation, a series of geometry optimizations were performed with bond constraints. Specifically, the bond distance between the target Cu and S atoms was constrained to vary between 1.0 and 4.0 Å in 0.2 Å steps for thioxocopper, and from 1.54 to 4.14 Å in 0.2 Å steps for $Cu(SCH_3)_2$. Similarly, the target Cu−S−C angle of the Cu (100)-thiol system was constrained to vary between 67.08° and 177.08° in 10° steps to calculate the energy curve for Cu−S−C; Figure 2 shows the results of these calculations. The maximum difference between the ReaxFF and QM Cu−S−C valence-angle energies (Figure 2a) was 2.7 kcal/mol, with ReaxFF slightly overpredicting this energy for angles larger and smaller than the equilibrium value. For the bond energies (Figure 2b and c), the most important feature is the energy between the minimum energy distance and that when the two atoms are far from one another, which describes the ability of ReaxFF to capture bonding and debonding. In this range, the force field can reproduce the results of the quantum calculations with a maximum energy difference of 25.3 and 4.2 kcal/mol for the Cu−S bond in thioxocopper (CuS) and the $Cu(SCH_3)_2$ molecule, respectively; near the energy minimum, the energy differences are significantly smaller.

The binding energies for S, thiol, and CH_3 adsorbed on Cu (100) are included in the training set to ensure that the new ReaxFF potential properly predicts the chemisorption energies of S, SCH_3, and CH_3 on the Cu surface. The binding energies (E_{bindng}) were calculated according to

$$E_{binding} = E_{slab} + E_{gas\text{-}phase\ absorbate} - E_{absorbate+slab} \quad (5)$$

where E_{slab} is the energy of a Cu (100) slab in vacuum and $E_{adsorbate+slab}$ is the energy of chemisorbed adsorbate on the Cu (100) surface after relaxation. The term $E_{gas\text{-}phase\ absorbate}$ is a reference energy for an isolated gas-phase absorbate species after relaxation. In some cases, binding energies were calculated with respect to stable gas-phase molecules and used to train the ReaxFF potential while, in other cases, energies were calculated with respect to the adsorbed radical in the gas phase to allow binding energies to be compared with previous work. From eq 5, a positive value of $E_{binding}$ indicates the adsorption is thermodynamically favorable, while a negative value indicates the chemisorption is thermodynamically unfavorable. To minimize interference from the periodic image of the adsorbate across the periodic boundary, the Cu (100) surface in our DFT and ReaxFF calculations consisted of 3 × 3 Cu atoms.[58]

Table 1 presents the binding energies on the Cu (100) surface calculated from QM and ReaxFF. Here, the energies of radicals were calculated from the binding energies of CH_3 and SCH_3, and the energy of octasulfur was used to calculate the binding energy of S. The most stable site for methyl thiolate adsorption is found to be the 4-fold hollow site, in agreement with experiment,[59] and the binding energy is also in good agreement with previous work.[60] The 2-fold bridge site is predicted to be the most stable position for a CH_3 group with a binding energy of ∼50 kcal/mol; which is within the range of values, 30.7 to 51.9 kcal/mol, reported from previous calculations of methyl species on Cu(111).[61] Shown in parentheses are the binding energies calculated with respect to dimethyl disulfide (DMDS) and C_2H_6 molecules as gas-phase references to establish the capability of the force field to properly calculate the binding energies of these species not only with respect to gas-phase radicals but also with respect to stable molecules. For an S atom, ReaxFF overpredicts the binding energy by between 5.8 and 7.1 kcal/mol, depending on the binding site. For the thiol and CH_3 molecules, ReaxFF underpredicts the binding energy by up to 25 kcal/mol. Importantly, the best match between ReaxFF and QM is observed for the binding sites that are the most stable, i.e., thiol on the 4-fold site, for which the energy difference is 2.6 kcal/mol, and the CH_3 on the 2-fold site, for which the energy difference is 4.9 kcal/mol.

Table 1. Binding Energies of S, CH_3, and SCH_3 on a Cu (100) Surface and Subsurface Sulfur Adsorption Energy[a]

geometry	ReaxFF energy (kcal/mol)	QM energy (kcal/mol)
S on Cu (100) 4-fold	51.75	45.93
S on Cu (100) 2-fold	32.16	25.90
S on Cu (100) 1-fold	14.60	7.46
thiol on Cu (100) 4-fold	66.34 (40.32)	68.98 (29.08)
thiol on Cu (100) 2-fold	38.64 (15.13)	52.64 (12.74)
thiol on Cu (100) 1-fold	17.19 (7.57)	37.5 (−2.4)
CH_3 on Cu (100) 4-fold	17.05 (−2.83)	42.75 (−8.83)
CH_3 on Cu (100) 2-fold	46.8 (0.27)	51.7 (−6.6)
CH_3 on Cu (100) 1-fold	39.32 (−41.2)	49.47 (−15.55)
subsurface adsorbed S	44.62	43.44

[a]Binding energies of CH_3 and methyl thiolate were calculated using radicals, while binding energy of S was calculated using an octasulfur molecule. Shown in parentheses are the energies calculated with respect to stable gas-phase molecules (ethane and DMDS).

DOI: 10.1021/acs.jpcb.7b06976
J. Phys. Chem. B XXXX, XXX, XXX−XXX

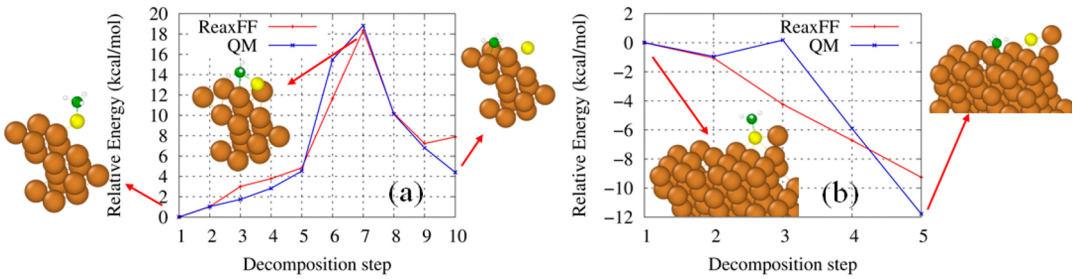

Figure 3. ReaxFF and QM energy curves for (a) methyl thiolate decomposition on an ideally flat Cu(100) surface, and (b) methyl thiolate decomposition on a Cu(100) surface with a vacancy and an adatom. The color scheme is the same as that in Figure 2.

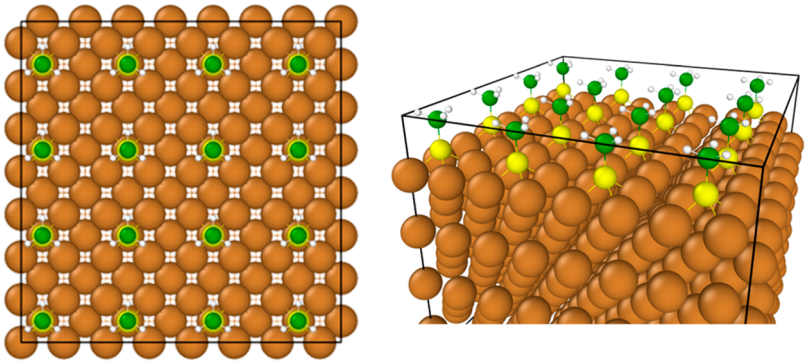

Figure 4. Top (left) and perspective views (right) of the configuration of the system used for the MD simulations in which 16 methyl thiolate species are deposited on a Cu (100) surface to provide a 0.25 ML coverage. The color scheme is the same as in Figure 2.

The process of methyl thiolate decomposition on the Cu(100) surface was also included in the training set. For this, the Vienna ab initio simulation package (VASP)[62,63] was used to calculate the energy barrier for decomposition of a methyl thiolate molecule on the Cu (100) surface using the nudged elastic band (NEB)[64,65] method. The PBE functional was applied, and the energy cutoff was 400 eV. Two NEB simulations were performed: one for the decomposition of methyl thiolate on an ideal Cu (100) surface, and one for the surface with an adatom and a vacancy. The results are shown in Figure 3. The maximum difference between ReaxFF and the energy calculated by DFT at any step in the decomposition of methyl thiolate on an ideal surface or one with a vacancy is 4.4 kcal/mol. Most energy differences are smaller than this, with the average difference for both surfaces being 1.3 kcal/mol.

MD Simulations of Thermal Reactions of Methyl Thiolate on Copper. To demonstrate the new ReaxFF potential's ability to describe thermal decomposition of methyl thiolate species on copper, a series of MD simulations were carried out to model the reactions that occur for methyl thiolate species on a Cu surface at different temperatures. The simulations calculate S−C bond dissociation because this reaction is the precursor to hydrocarbon formation, which has been measured experimentally in previous temperature-programmed desorption (TPD) experiments.[66] In the experiments, methyl thiolate species thermally decomposed and then reacted to desorb small hydrocarbons (methane, ethylene, and ethane) with a peak desorption temperature of ∼425 K in TPD, corresponding to a reaction activation energy of ∼24 kcal/mol, to leave chemisorbed sulfur on the surface. However, significantly higher simulation temperatures were used here to accelerate the reaction rates to allow reaction events to be observed on the time scale of the simulation.

The system configuration used for the simulation is shown in Figure 4 and consisted of a Cu vacuum slab with a Cu (100) surface that is 8 layers thick, with 512 Cu atoms. A total of 16 methyl thiolate species were deposited on the surface to yield a 0.25 monolayer (ML) coverage, where the coverage was measured relative to the number of copper atoms on the (100) surface.

The simulations were run for 6 ns at 400, 500, 600, and 700 K, with a 0.25 fs time step in the NVT ensemble (with a constant number of atoms, volume, and temperature). The TPD experiments ramped the temperature from 100 to 700 K using a 4.2 K/s heating rate.[66] This heating rate can be approximated as isothermal on the MD simulation time scale, since 4.2 K/s represents 4.2×10^{-9} K/ns, which corresponds to a negligible temperature variation during the 6 ns simulation time.

During each simulation, the decomposition of the methyl thiolate species on the surface was characterized by monitoring the number of methyl thiolate species in which the C−S bond order was reduced below a value of 0.2. Figure 5 represents the number of dissociated methyl species (CH_3) from thiolate molecules after S−C bond scission. It is observed that the fewest dissociation events occurred at the lowest temperature of 400 K, where only temporary scission of Cu−S bonds occurred due to thermal fluctuations. It is also observed that, during the initial 1 ns of simulation time, decomposition occurred more slowly at 500 K than the other two higher temperatures. An increased reaction rate with increasing temperature is expected, and was demonstrated for this system in previously reported TPD experiments of dimethyl disulfide on copper.[66] In the TPD experiments, the amount of methane was detected, while in the simulation we counted S−C bond dissociation events. However, the trends in these two metrics can be compared

DOI: 10.1021/acs.jpcb.7b06976
J. Phys. Chem. B XXXX, XXX, XXX−XXX

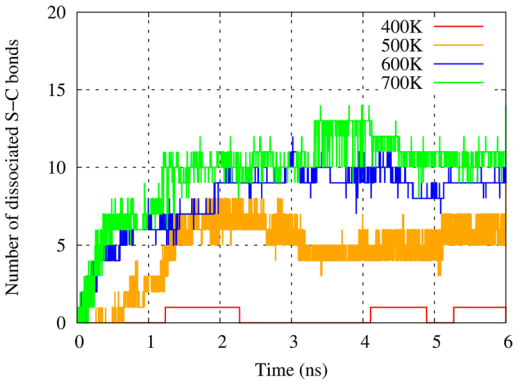

Figure 5. Number of thiols that decomposed on the Cu(100) surface as a function of time during 6 ns MD simulations at different temperatures.

because bond dissociation is the first step toward the formation of methane in the experiments.

According to the data in Figure 5, at temperatures of 500, 600, and 700 K, S–C bond dissociation reaches steady state, i.e., the number of bonds oscillates about a constant value, after the first 2 ns of the simulation. This implies that the process of S–C bond scission is reversible on this short time scale such that some S–C bonds break and then reform, although not necessarily between the same two atoms, as shown next. In order to explore this effect, Figure 6 shows the trajectory of the

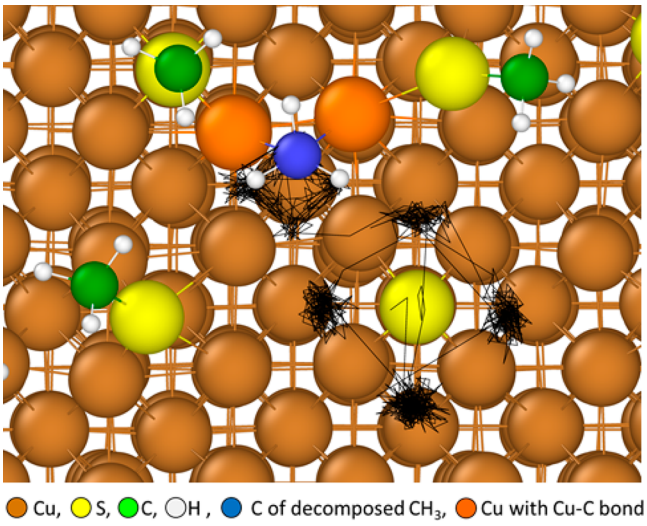

Figure 6. Trajectory (black line) of the carbon (blue sphere) of an adsorbed CH_3 species on Cu (100). The blue carbon identifies that the methyl group has now diffused away from the chemisorbed sulfur atom to bind at a copper bridge site.

carbon atom from a CH_3 molecule from the 400 K simulation. Consistent with the DFT data, the ReaxFF simulations show that adsorbed CH_3 species prefer the bridge adsorption site on Cu (100). The methyl group remains in the vicinity of the sulfur atom, in some cases diffusing across it, presumably to transiently reform the methyl thiolate species.

Figure 7 summarizes the processes occurring during methyl thiolate decomposition on Cu (100) observed in the 400 K MD simulation. From the initially chemisorbed SCH_3 species (Figure 7a), the C–S bonds tilt causing the CH_3 group to approach the surface (as highlighted by the blue carbon atom),

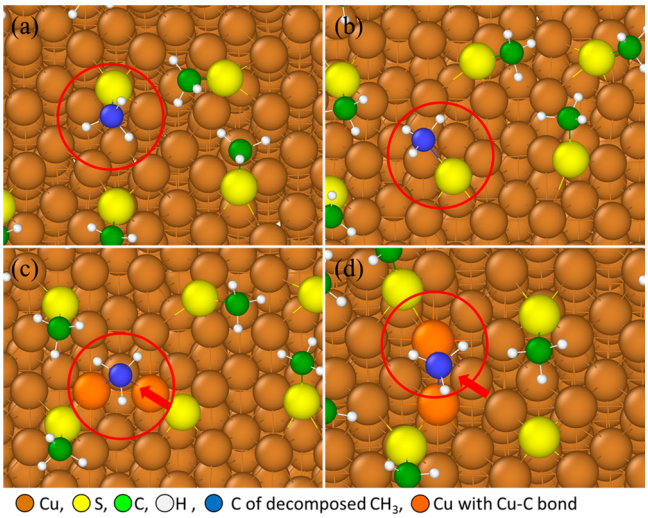

Figure 7. Process of thiol decomposition on a Cu (100) surface. (a) Chemisorbed methyl thiolate species on a Cu (100) surface, (b) the motion of the CH_3 group close to the surface, (c) the completion of methyl thiolate decomposition showing CH_3 binding to adjacent Cu sites, (d) CH_3 diffusion on the Cu (100) surface. In each image, the red circle identifies the most relevant atoms and red arrows indicate motion direction.

resulting in a small surface–S–C angle, as shown in Figure 7b. Then, as shown in Figure 7c, C–S bond scission occurs causing the resulting CH_3 species to move to a copper atom on the surface. Lastly, as shown in Figure 7d, the CH_3 group diffuses on the surface away from the remaining sulfur atom. This CH_3 is the precursor to small hydrocarbon formation observed in TPD experiments and consistent with the formation of ethane resulting from the coupling between two methyl groups. The simulation was not run for a sufficiently long time to observe the fate of the resulting methyl species. Nevertheless, the simulations accurately capture the products in the experimentally observed surface reaction pathway as measured by TPD.[66]

During the MD simulation, reattachment of CH_3 groups to S atoms was observed. Figure 8 shows a S–C bond-breaking event and successive migration of a CH_3 species to another adsorbed S atom, forming a new methyl thiolate species on the Cu (100) surface at 500 K. The process begins from a S–C bond dissociation of one of the adsorbed methyl thiolates in Figure 8a. Another S–C bond dissociation event occurs, leaving two S atoms and two CH_3 species adsorbed on the Cu (100) surface in Figure 8b. One of the roaming CH_3 species approaches an adjacent sulfur atom in Figure 8c. Lastly, a new thiol molecule is formed as a S–C bond is reestablished (Figure 8d). This CH_3 migration and subsequent methyl thiolate formation occurred at 500, 600, and 700 K, throughout the 6 ns of the simulation. The reattachment of S–C bonds explains the stabilization of the number of dissociated S–C bonds after 2–3 ns of simulation time shown in Figure 5.

Lastly, in order to explore the subsequent reaction pathways, a surface was created with a methyl species adsorbed on a surface containing methyl thiolate species and a simulation was carried out at 700 K to accelerate the reaction rates. The results of the simulated reaction sequence are shown in Figure 9. As shown in Figure 9a, the process starts with chemisorbed methyl thiolate species and an adsorbed CH_3 group on the Cu (100) surface. The methyl thiolate species reacts by C–S bond

DOI: 10.1021/acs.jpcb.7b06976
J. Phys. Chem. B XXXX, XXX, XXX–XXX

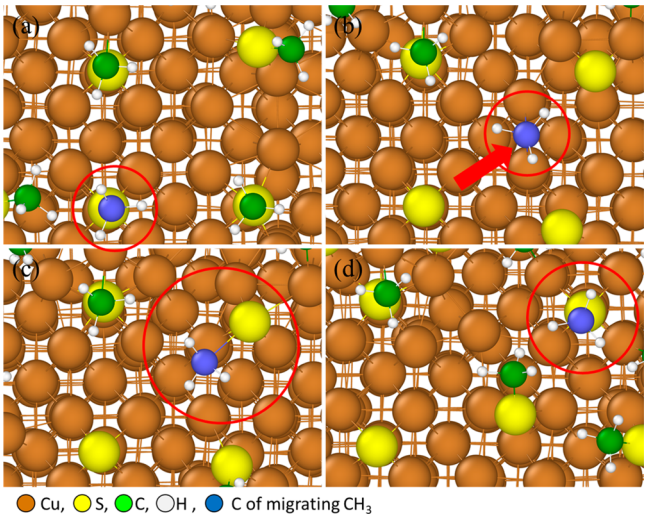

Figure 8. Process of CH_3 migration on Cu (100) surface: (a) The CH_3 group (C atom highlighted in blue) is unstable, and about to dissociated from the S atom; (b) S−C bond dissociation occurs; (c) the target CH_3 migrates on the Cu(100) surface approaching another S atom; and (d) a new methyl thiolate species is formed. In each image, the red circle identifies the most relevant atoms and red arrows indicate motion direction.

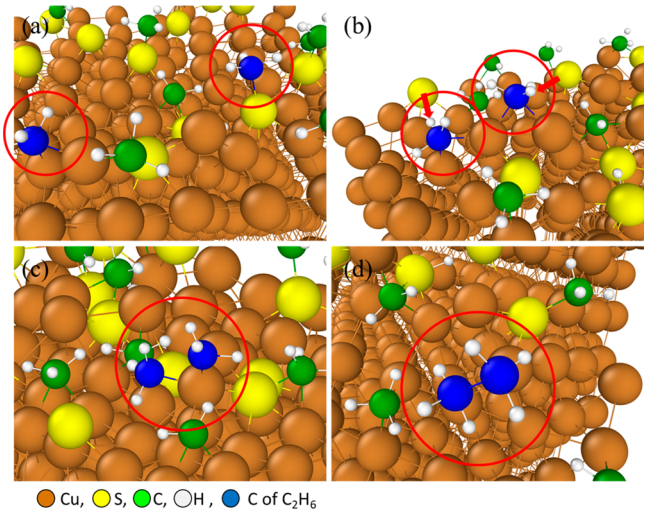

Figure 9. Process of ethane formation on the Cu (100) surface. (a) Chemisorbed methyl thiolate species and an adsorbed CH_3 group on a Cu (100) surface (relevant carbon atoms highlighted in blue); (b) the methyl thiolate decomposes to form two adsorbed methyl species; (c) the methyl species diffuse to bind to adjacent copper atoms on the surface; and (d) C_2H_6 forms from a reaction between the methyl species on Cu(100) and then rapidly desorbs. In each image, the red circle identifies the most relevant atoms and red arrows indicate motion direction.

scission, as discussed above, to form another methyl species and adsorbed sulfur, to yield two CH_3 groups that are bonded on the Cu surface, as shown in Figure 9b. The two CH_3 species diffuse rapidly toward each other at 700 K, forming a metastable Cu-2CH_3 state for a very short time in Figure 9c. Finally, in Figure 9d, ethane is formed and rapidly desorbs from the Cu surface. These results demonstrate that the current ReaxFF potential can be used to model both methyl thiolate decomposition and subsequent hydrocarbon formation reaction pathways.

It should be noted that methane is also formed in the thermal and tribochemical reactions. However, this subsequent step would require the dehydrogenation by the transfer of hydrogen from one methyl group to the other to form an adsorbed CH_2 species that presumably combine to form ethylene, which is found in the thermal reaction. However, the activation barriers for these processes are not included in the database for the ReaxFF training set.

CONCLUSIONS

In this work, DFT simulations were performed and used to train ReaxFF parameters to develop a new Cu/S potential to describe the thermal reactions of alkyl thiolate species on Cu surfaces. The parametrization process included volumetric expansion/compression of CuS, CuS_2, and Cu_2S unit cells; bond dissociation of Cu−S and valence angle bending of Cu−S−C; the binding energy of SCH_3, CH_3, and S atoms; and energy curves for the decomposition of methyl thiolate species on copper.

MD simulations were performed to demonstrate the ability of the new force field to describe experimentally observed methyl thiolate-Cu surface chemistry and Cu−S interactions. MD simulations carried out for 6 ns at 400, 500, 600, and 700 K showed that the current Cu/S potential can capture methyl thiolate decomposition that increases with temperature, similar the observations from TPD experiments. In addition, we observed the process of thiol decomposition and ethane formation on a Cu (100) surface, which demonstrates the potential's ability to simulate the surface chemistry and hydrocarbon formation of Cu−S and Cu−alkyl thiolate systems. These reactive potentials can be used in the future to investigate the chemistry induced at a sliding interface to explore how the reaction rate varies with the forces exerted on the adsorbed alkyl thiolate species to test whether they obey the simple Bell model (eq 1) and to provide estimates of the value of the activation length $\Delta x^{\ddagger}$ to compare with experiment.

ASSOCIATED CONTENT

Supporting Information

The Supporting Information is available free of charge on the ACS Publications website at DOI: 10.1021/acs.jpcb.7b06976.

ReaxFF parameters for Cu/S/C/H developed in this (TXT)

AUTHOR INFORMATION

Corresponding Author

*E-mail: amartini@ucmerced.edu.

ORCID

Jejoon Yeon: 0000-0001-6323-7572
Wilfred T. Tysoe: 0000-0002-9295-448X
Ashlie Martini: 0000-0003-2017-6081

Notes

The authors declare no competing financial interest.

ACKNOWLEDGMENTS

We greatly appreciate the National Science Foundation for financial support through grant numbers CMMI-1634354 and CMMI-1634340.

DOI: 10.1021/acs.jpcb.7b06976
J. Phys. Chem. B XXXX, XXX, XXX−XXX

REFERENCES

(1) Eilert, A.; Roberts, F. S.; Friebel, D.; Nilsson, A. Formation of Copper Catalysts for CO_2 Reduction with High Ethylene/Methane Product Ratio Investigated with in Situ X-Ray Absorption Spectroscopy. *J. Phys. Chem. Lett.* **2016**, *7* (8), 1466−1470.

(2) Lindström, B. Hydrogen Generation by Steam Reforming of Methanol over Copper-Based Catalysts for Fuel Cell Applications. *Int. J. Hydrogen Energy* **2001**, *26* (9), 923−933.

(3) Raeymaekers, B.; Lee, D. E.; Talke, F. E. A Study of the Brush/rotor Interface of a Homopolar Motor Using Acoustic Emission. *Tribol. Int.* **2008**, *41* (5), 443−448.

(4) Jia, J.; Bendounan, A.; Chaouchi, K.; Esaulov, V. A. Sulfur Interaction with Cu(100) and Cu(111) Surfaces: A Photoemission Study. *J. Phys. Chem. C* **2014**, *118* (42), 24583−24590.

(5) Scherer, J.; Vogt, M. R.; Magnussen, O. M.; Behm, R. J. Corrosion of Alkanethiol-Covered Cu(100) Surfaces in Hydrochloric Acid Solution Studied by in-Situ Scanning Tunneling Microscopy. *Langmuir* **1997**, *13* (26), 7045−7051.

(6) Keller, H.; Simak, P.; Schrepp, W.; Dembowski, J. Surface Chemistry of Thiols on Copper: An Efficient Way of Producing Multilayers. *Thin Solid Films* **1994**, *244* (1−2), 799−805.

(7) Knickelbein, M. B. Reactions of Transition Metal Clusters with Small Molecules. *Annu. Rev. Phys. Chem.* **1999**, *50*, 79−115.

(8) Pakiari, A. H.; Jamshidi, Z. Interaction of Coinage Metal Clusters with Chalcogen Dihydrides. *J. Phys. Chem. A* **2008**, *112* (34), 7969−7975.

(9) Ghebriel, H. W.; Kshirsagar, A. Adsorption of Molecular Hydrogen and Hydrogen Sulfide on Au Clusters. *J. Chem. Phys.* **2007**, *126* (24), 244705.

(10) Vahrenkamp, H. Sulfur Atoms as Ligands in Metal Complexes. *Angew. Chem., Int. Ed. Engl.* **1975**, *14* (5), 322−329.

(11) Kennedy, B. P.; Lever, A. B. P. Studies of the Metal−Sulfur Bond. Complexes of the Pyridine Thiols. *Can. J. Chem.* **1972**, *50*, 3488.

(12) Pakiari, A.; Jamshidi, Z. Nature and Strength of M− S Bonds (M= Au, Ag, and Cu) in Binary Alloy Gold Clusters. *J. Phys. Chem. A* **2010**, *114*, 9212−9221.

(13) Blunt, T. J.; Kotvis, P. V.; Tysoe, W. T. Determination of Interfacial Temperatures under Extreme Pressure Conditions. *Tribol. Lett.* **1996**, *2* (3), 221−230.

(14) Kotvis, P. V.; Tysoe, W. T. Surface Chemistry of Chlorinated Hydrocarbon Lubricant Additives − Part I: Extreme-Pressure Tribology. *Tribol. Trans.* **1998**, *41*, 117−123.

(15) Blunt, T. J.; Kotvis, P. V.; Tysoe, W. T. Surface Chemistry of Chlorinated Hydrocarbon Lubricant Additives − Part II: Modeling the Tribological Interface. *Tribol. Trans.* **1998**, *41*, 129−139.

(16) Lara, J.; Surerus, K. K.; Kotvis, P. V.; Contreras, M. E.; Rico, J. L.; Tysoe, W. T. The Surface and Tribological Chemistry of Carbon Disulfide as an Extreme-Pressure Additive. *Wear* **2000**, *239*, 77−82.

(17) Kaltchev, M.; Kotvis, P. V.; Blunt, T. J.; Lara, J.; Tysoe, W. T. A Molecular Beam Study of the Tribological Chemistry of Dialkyl Disulfides. *Tribol. Lett.* **2001**, *10* (1), 45−50.

(18) Gao, F.; Furlong, O.; Kotvis, P. V.; Tysoe, W. T. Tribological Properties of Films Formed by the Reaction of Carbon Tetrachloride with Iron. *Tribol. Lett.* **2005**, *20* (2), 171−176.

(19) Zhang, J.; Spikes, H. On the Mechanism of ZDDP Antiwear Film Formation. *Tribol. Lett.* **2016**, *63* (2), 1−15.

(20) Felts, J. R.; Oyer, A. J.; Hernandez, S. C.; Whitener, K. E., Jr; Robinson, J. T.; Walton, S. G.; Sheehan, P. E. Direct Mechanochemical Cleavage of Functional Groups from Graphene. *Nat. Commun.* **2015**, *6*, 6467.

(21) Gosvami, N. N.; Bares, J. A.; Mangolini, F.; Konicek, A. R.; Yablon, D. G.; Carpick, R. W. Mechanisms of Antiwear Tribofilm Growth Revealed in Situ by Single-Asperity Sliding Contacts. *Science* **2015**, *348* (6230), 102−106.

(22) Adams, H. L.; Garvey, M. T.; Ramasamy, U. S.; Ye, Z.; Martini, A.; Tysoe, W. T. Shear-Induced Mechanochemistry: Pushing Molecules Around. *J. Phys. Chem. C* **2015**, *119*, 7115.

(23) Adams, H.; Miller, B. P.; Kotvis, P. V.; Furlong, O. J.; Martini, A.; Tysoe, W. T. Situ Measurements of Boundary Film Formation Pathways and Kinetics: Dimethyl and Diethyl Disulfide on Copper. *Tribol. Lett.* **2016**, *62* (1), 1−9.

(24) Furlong, O. J.; Miller, B. P.; Kotvis, P.; Tysoe, W. T. Low-Temperature, Shear-Induced Tribofilm Formation from Dimethyl Disulfide on Copper. *ACS Appl. Mater. Interfaces* **2011**, *3*, 795−800.

(25) Furlong, O. J.; Miller, B. P.; Tysoe, W. T. Shear-Induced Surface-to-Bulk Transport at Room Temperature in a Sliding Metal − Metal Interface. *Tribol. Lett.* **2011**, *41*, 257−261.

(26) Furlong, O.; Miller, B.; Tysoe, W. T. Shear-Induced Boundary Film Formation from Dialkyl Sulfides on Copper. *Wear* **2012**, *274−275*, 183−187.

(27) Miller, B.; Furlong, O.; Tysoe, W. T. The Kinetics of Shear-Induced Boundary Film Formation from Dimethyl Disulfide on Copper. *Tribol. Lett.* **2013**, *49*, 39−46.

(28) Bell, G. Models for the Specific Adhesion of Cells to Cells. *Science* **1978**, *200*, 618−627.

(29) Eyring, H. The Activated Complex in Chemical Reactions. *J. Chem. Phys.* **1935**, *3* (2), 107−115.

(30) Spikes, H.; Tysoe, W. On the Commonality Between Theoretical Models for Fluid and Solid Friction, Wear and Tribochemistry. *Tribol. Lett.* **2015**, *59*, 21.

(31) Hu, X.; Altoe, M. V. P.; Martini, A. Amorphization-Assisted Nanoscale Wear during the Running-in Process. *Wear* **2017**, *370−371* (15), 46−50.

(32) Dong, Y.; Li, Q.; Martini, A. Molecular Dynamics Simulation of Atomic Friction: A Review and Guide. *J. Vac. Sci. Technol., A* **2013**, *31* (3), 030801.

(33) Yeon, J.; He, X.; Martini, A.; Kim, S. H. Mechanochemistry at Solid Surfaces: Polymerization of Adsorbed Molecules by Mechanical Shear at Tribological Interfaces. *ACS Appl. Mater. Interfaces* **2017**, *9* (3), 3142−3148.

(34) van Duin, A. C. T.; Dasgupta, S.; Lorant, F.; Goddard, W. a. ReaxFF: A Reactive Force Field for Hydrocarbons. *J. Phys. Chem. A* **2001**, *105* (41), 9396−9409.

(35) Järvi, T. T.; Van Duin, A. C. T.; Nordlund, K.; Goddard, W. A. Development of Interatomic ReaxFF Potentials for Au-S-C-H Systems. *J. Phys. Chem. A* **2011**, *115* (37), 10315−10322.

(36) Voter, A. F. Parallel Replica Method for Dynamics of Infrequent Events. *Phys. Rev. B: Condens. Matter Mater. Phys.* **1998**, *57* (22), R13985−R13988.

(37) Martini, A.; Dong, Y.; Perez, D.; Voter, A. F. Low-Speed Atomistic Simulation of Stick − Slip Friction Using Parallel Replica Dynamics. *Tribol. Lett.* **2009**, *36*, 63−68.

(38) Joshi, K. L.; Raman, S.; van Duin, A. C. T. Connectivity-Based Parallel Replica Dynamics for Chemically Reactive Systems: From Femtoseconds to Microseconds. *J. Phys. Chem. Lett.* **2013**, *4*, 3792−3797.

(39) Li, Q.; Dong, Y.; Perez, D.; Martini, A.; Carpick, R. W. Speed Dependence of Atomic Stick-Slip Friction in Optimally Matched Experiments and Molecular Dynamics Simulations. *Phys. Rev. Lett.* **2011**, *106*, 126101.

(40) Liu, X.-Z.; Ye, Z.; Dong, Y.; Egberts, P.; Carpick, R. W.; Martini, A. Dynamics of Atomic Stick-Slip Friction Examined with Atomic Force Microscopy and Atomistic Simulations at Overlapping Speeds. *Phys. Rev. Lett.* **2015**, *114*, 146102.

(41) van Duin, A. C. T.; Baas, J. M. A.; van de Graaf, B. Delft Molecular Mechanics A New Approach to Hydrocarbon Force Fields. *J. Chem. Soc., Faraday Trans.* **1994**, *90* (19), 2881−2895.

(42) Islam, M. M.; Ostadhossein, A.; Borodin, O.; Yeates, A. T.; Tipton, W. W.; Hennig, R. G.; Kumar, N.; van Duin, A. C. T. ReaxFF Molecular Dynamics Simulations on Lithiated Sulfur Cathode Materials. *Phys. Chem. Chem. Phys.* **2015**, *17* (5), 3383−3393.

(43) Van Duin, A. C. T; Strachan, A.; Stewman, S.; Zhang, Q.; Xu, X.; Goddard, W. A. *Reactive Force Field for Silicon and Silicon Oxide Systems*; 2003; No. *1*, pp 3803−3811.

(44) Nielson, K. D.; Van Duin, A. C. T.; Oxgaard, J.; Deng, W. Q.; Goddard, W. A. Development of the ReaxFF Reactive Force Field for Describing Transition Metal Catalyzed Reactions, with Application to

DOI: 10.1021/acs.jpcb.7b06976
J. Phys. Chem. B XXXX, XXX, XXX−XXX

the Initial Stages of the Catalytic Formation of Carbon Nanotubes. *J. Phys. Chem. A* **2005**, *109* (3), 493−499.
(45) Mortier, W. J.; Ghosh, S. K.; Shankar, S. Electronegativity-Equalization Method for the Calculation of Atomic Charges in Molecules. *J. Am. Chem. Soc.* **1986**, *108* (15), 4315−4320.
(46) Chenoweth, K.; van Duin, A. C. T.; Goddard, W. A. ReaxFF Reactive Force Field for Molecular Dynamics Simulations of Hydrocarbon Oxidation. *J. Phys. Chem. A* **2008**, *112* (5), 1040−1053.
(47) Becke, A. D. Density-functional Thermochemistry. III. The Role of Exact Exchange. *J. Chem. Phys.* **1993**, *98* (7), 5648−5652.
(48) Becke, A. D. Density-Functional Exchange-Energy Approximation with Correct Asymptotic Behavior. *Phys. Rev. A: At., Mol., Opt. Phys.* **1988**, *38* (6), 3098−3100.
(49) Lee, C.; Yang, W.; Parr, R. G. Development of the Colle-Salvetti Correlation-Energy Formula into a Functional of the Electron Density. *Phys. Rev. B: Condens. Matter Mater. Phys.* **1988**, *37* (2), 785−789.
(50) Francl, M. M.; Pietro, W. J.; Hehre, W. J.; Binkley, J. S.; Gordon, M. S.; DeFrees, D. J.; Pople, J. A. Self-consistent Molecular Orbital Methods. XXIII. A Polarization-type Basis Set for Second-row Elements. *J. Chem. Phys.* **1982**, *77* (7), 3654−3665.
(51) Giannozzi, P.; Baroni, S.; Bonini, N.; Calandra, M.; Car, R.; Cavazzoni, C.; Ceresoli, D.; Chiarotti, G. L.; Cococcioni, M.; Dabo, I.; et al. Quantum ESPRESSO: A Modular and Open-Source Software Project for Quantum Simulations of Materials. *J. Phys.: Condens. Matter* **2009**, *21*, 395502.
(52) Perdew, J. P.; Burke, K.; Ernzerhof, M. Generalized Gradient Approximation Made Simple. *Phys. Rev. Lett.* **1996**, *77* (18), 3865−3868.
(53) Vanderbilt, D. Soft Self-Consistent Pseudopotentials in a Generalized Eigenvalue Formalism. *Phys. Rev. B: Condens. Matter Mater. Phys.* **1990**, *41* (11), 7892−7895.
(54) Rappe, A. M.; Rabe, K. M.; Kaxiras, E.; Joannopoulos, J. D. Optimized Pseudopotentials. *Phys. Rev. B: Condens. Matter Mater. Phys.* **1990**, *41* (2), 1227−1230.
(55) Monkhorst, H. J.; Pack, J. D. Special Points for Brillonin-Zone Integrations. *Phys. Rev. B* **1977**, *16* (4), 1748−1749.
(56) Chadi, D. J.; Cohen, M. L. Special Points in the Brillouin Zone. *Phys. Rev. B* **1973**, *8* (12), 5747−5753.
(57) Rahaman, O.; Van Duin, A. C. T.; Bryantsev, V. S.; Mueller, J. E.; Solares, S. D.; Goddard, W. A.; Doren, D. J. Development of a ReaxFF Reactive Force Field for Aqueous Chloride and Copper Chloride. *J. Phys. Chem. A* **2010**, *114* (10), 3556−3568.
(58) Malyi, O. I.; Bai, K.; Kulish, V. V.; Wu, P.; Chen, Z. Density Functional Theory Study of Sulfur Tolerance of Copper: New Copper-Sulfur Phase Diagram. *Chem. Phys. Lett.* **2012**, *533*, 20−24.
(59) Kariapper, M. S.; Fisher, C.; Woodruff, D. P.; Cowie, B. C. C.; Jones, R. G. A Structural Study of Methanethiolate Adsorbed on Cu(100). *J. Phys.: Condens. Matter* **2000**, *12* (10), 2153−2161.
(60) Ferral, A.; Patrito, E. M.; Paredes-Olivera, P. Structure and Bonding of Alkanethiols on Cu (111) and Cu (100). *J. Phys. Chem. B* **2006**, *110*, 17050−17062.
(61) Wang, G.; Li, J.; Xu, X.; Li, R.; Nakamura, J. The Relationship Between Adsorption Energies of Methyl on Metals and the Metallic Electronic Properties: A First-Principles DFT Study. *J. Comput. Chem.* **2005**, *26*, 871−878.
(62) Kresse, G.; Hafner, J. Ab Initio Molecular Dynamics for Liquid Metals. *Phys. Rev. B: Condens. Matter Mater. Phys.* **1993**, *47* (1), 558−561.
(63) Kresse, G.; Hafner, J. Ab Initio Molecular Dynamics for Open-Shell Transition Metals. *Phys. Rev. B: Condens. Matter Mater. Phys.* **1993**, *48* (17), 13115−13118.
(64) Mills, G.; Jonsson, H. Quantum and Thermal Effects in H2 Dissociative Adsorption: Evaluation of Free Energy Barriers in Multidimensional Quantum Systems. *Phys. Rev. Lett.* **1994**, *72* (7), 1124−1127.
(65) Mills, G.; Jonsson, H.; Schenter, G. K. Reversible Work Transiton State Theory: Application to Dissociative Adsorption of Hydrogen. *Surf. Sci.* **1995**, *324*, 305−337.
(66) Furlong, O. J.; Miller, B. P.; Li, Z.; Walker, J.; Burkholder, L.; Tysoe, W. T. The Surface Chemistry of Dimethyl Disulfide on Copper. *Langmuir* **2010**, *26* (21), 16375−16380.

DOI: 10.1021/acs.jpcb.7b06976
J. Phys. Chem. B XXXX, XXX, XXX−XXX